

Differential Cross Section of the $pn \rightarrow pp(^1S_0)\pi^-$ Reaction Extracted from $pd \rightarrow ppp\pi^-$

F. Duncan,¹ H. Hahn,³ C. Aclander,³ D. Ashery,³ E. G. Auld,² D. R. Gill,⁴ D. A. Hutcheon,⁴ G. Jones,²
 E. Korkmaz,⁵ S. Maytal-Beck,³ M. A. Moinester,³ J. A. Niskanen,⁶ D. Ottewell,⁴ A. Rahav,³ S. Ram,³
 M. Sevier,⁷ P. L. Walden,⁴ and R. Weiss³

¹*Department of Physics, Queen's University, Kingston, Ontario, Canada K7L 3N6*

²*Department of Physics, University of British Columbia, Vancouver, British Columbia, Canada V6T 1Z1*

³*Raymond and Beverly Sackler Faculty of Exact Sciences, School of Physics and Astronomy,
 Tel-Aviv University, 69978 Ramat Aviv, Israel*

⁴*TRIUMF, 4004 Wesbrook Mall, Vancouver, British Columbia, Canada V6T 2A3*

⁵*Department of Physics, University of Northern British Columbia, Prince George, British Columbia, Canada V2L 5P2*

⁶*Department of Physics, University of Helsinki, P.O. Box 9, FIN-00014 Finland*

⁷*School of Physics, University of Melbourne, Parkville, Victoria, Australia 3052*

(Received 18 December 1997)

The double differential cross section for $pn \rightarrow pp(^1S_0)\pi^-$ at three beam energies has been extracted from the quasifree process $pd \rightarrow ppp\pi^-$. A comparison is carried out with single differential cross section measurements for ${}^3\text{He}(\pi^-, pn)n$, where the pion is thought to be absorbed onto a $pp(^1S_0)$ "diproton" state. A significant difference is observed in the shape of the angular distribution between the production and absorption data. This difference is ascribed to the effects of the ${}^3\text{He}$ nuclear environment characterizing the absorption process; however, an adequate theoretical explanation is not available. [S0031-9007(98)06103-1]

PACS numbers: 13.75.Cs, 25.10.+s, 25.40.Qa, 25.80.Ls

The $pn \leftrightarrow pp\pi^-$ reaction is interesting because, in addition to involving the isospin one channel which permits the formation of an intermediate $N\Delta$ state, it also includes the nonresonant isospin zero channel where the $N\Delta$ state is forbidden. It is common to refer to the relevant cross sections as the σ_{11} and σ_{01} channels (the subscripts referring to the initial and final NN isospin state) [1]. The nonresonant σ_{01} channel can be enhanced relative to the resonant σ_{11} channel by restricting the final state protons of the $pn \rightarrow pp\pi^-$ reaction to a ${}^{2S+1}L_j = {}^1S_0$ state [in the rest of the paper, this $pp(^1S_0)$ state is referred to as a "diproton"]. Such a restriction prevents the $N\Delta$ transitions from 1D_2 and 3F_3 , the two nucleon initial states that dominate the $\sigma_{10}(pp \rightarrow d\pi^+)$ process, from contributing to the σ_{11} channel. Thus, the reaction $pn \rightarrow pp(^1S_0)\pi^-$ is expected to be particularly sensitive to the normally weak nonresonant pion production mechanism.

Most studies of $pn \rightarrow pp(^1S_0)\pi^-$ reactions have been carried out through the ${}^3\text{He}(\pi^-, pn)n$ reaction in a kinematical regime where the pion is absorbed onto a bound diproton [2–5]. A partial wave amplitude analysis of $T_\pi = 62.5$ MeV ${}^3\text{He}(\pi^-, pn)n$ differential cross section data [3] by Piasetzky *et al.* [6] (which included only s - and p -wave pion partial waves) yielded two distinct solutions. Both solutions indicate that less than 7% of the total reaction cross section arises from absorption through the single s -wave pion channel (which is the only σ_{11} transition allowed for s - and p -wave pions), thus suggesting that the $pn \rightarrow pp(^1S_0)\pi^-$ reaction proceeds primarily through the nonresonant isospin zero channel.

The two solutions, which differ in terms of the relative contributions of the two p -wave pion amplitudes, could

be distinguished by analyzing power measurements using a polarized initial state nucleon for the pion production reaction $pn \rightarrow pp(^1S_0)\pi^-$. Ponting *et al.* [7] carried out such a measurement by isolating the quasifree $\vec{p}n \rightarrow pp(^1S_0)\pi^-$ reaction from $\vec{p}d \rightarrow ppp\pi^-$. Although the measured analyzing power was in qualitative agreement with one of the two Piasetzky *et al.* solutions, the measured analyzing power had a zero crossing angle which was not consistent with the minima of the absorption cross section. This inconsistency precluded any possibility of having any partial wave solution based both on the ${}^3\text{He}$ cross section and the $\vec{p}d \rightarrow ppp\pi^-$ analyzing power.

The observed discrepancy could be due either to experimental error or to the fact that the production process and the absorption process are two significantly different reactions. To resolve this discrepancy, we have completed a more extensive measurement of the $\vec{p}d \rightarrow ppp\pi^-$ reaction, extracting both double differential cross sections and analyzing powers. The experiment was similar to that of Ponting *et al.* [7] but with improvements in technique and hardware. The data were taken at three proton beam energies, 353, 403, and 440 MeV corresponding to an η_π of 0.66, 0.92, and 1.06, respectively, where $\eta_\pi = P_\pi^*/M_\pi$ and P_π^* is the pion momentum in the $pp\pi^-$ c.m. frame. The cross section data are reported in this Letter. The analyzing power data are presented separately [8].

The experiment was conducted on the 1B beam line at TRIUMF. The target was an upright 5 cm diameter aluminum cylinder containing liquid deuterium. The pions were detected in the TRIUMF quad-quad-dipole (QQD) spectrometer [9] operated with its front quadrupole removed. Position-sensitive information was obtained from

four wire chambers. One chamber upstream and one downstream of the quadrupole provided target traceback. The remaining two, placed after the 70° bend dipole, provided information on the momentum of the particle. QGD events were triggered by a triple coincidence between a start scintillator (ST), located before the first wire chamber, and two banks of scintillators placed after the wire chambers following the dipole. Candidate diprotons were detected in a $1\text{ m} \times 1\text{ m}$ scintillator wall (hodoscope) [2] located 400 cm downstream of the target, centered at an angle of 10° from the beam. The wall consisted of eight bars, each 12.5 cm square and 1 m tall equipped with a photomultiplier (PM) at either end. Timing was obtained from time-to-digital converters (TDC's) started by the pion firing the ST counter and stopped by protons firing the bar PM's. Proton energy was determined by the time-of-flight obtained from the sum of the TDC's, and vertical position along the bar was obtained from the difference between the TDC's. Veto counters were located behind the proton bar array to reject the fast protons which were able to penetrate the array. The hardware trigger required signals from at least two bars firing with no corresponding veto counters, an "EXIT" counter placed at the target exit window in front of the bars, and the QGD signal. Beam current was monitored to 4% systematic uncertainty with a secondary emission monitor which was calibrated against a Faraday cup. Beam intensity was maintained between 0.1 and 0.5 nA, limited by the single rates in the QGD wire chambers. Background measurements were carried out with both an empty target to check background from the target walls (there was none), and with QGD angles and magnetic field set to values incompatible with quasifree kinematics to check background from the four-body reaction $d(\vec{p}, ppp\pi^-)$ (no significant signal was detected).

In off-line analysis various cuts were imposed to clean up the event sample. Cuts were placed on wire chamber apertures, proton times-of-flight, and events where the vertical separation in adjacent bars was < 10 cm. The last cut eliminated events where a proton entered one bar and scattered into an adjacent one. Corrections due to $\pi \rightarrow \mu\nu$ decays were included in the Monte Carlo acceptance calculation. Events from $pd \rightarrow ppp\pi^-$ were identified by reconstructing T_{diff} , the energy difference between the initial pd and final $ppp\pi^-$ states. Figure 1 shows a typical T_{diff} histogram. It has three components, a peak near zero due to good $pd \rightarrow ppp\pi^-$ events, an additional peak at 30 MeV, and an underlying background. The peak near 30 MeV is due to events where one of the protons passes through the body of the target chamber rather than through the window (the EXIT counter required at least one proton to exit the window). The peaks were fitted to Gaussians and the background to a fourth order polynomial. The maximum fraction of background under the peak was 20% of the peak yield, and the maximum change of the peak

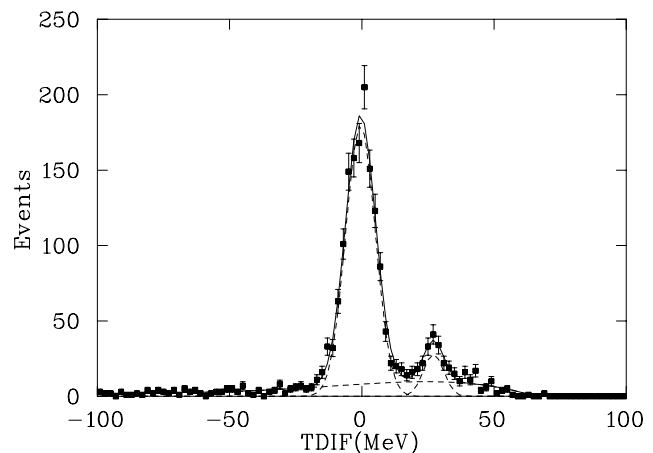


FIG. 1. Experimental T_{diff} for $pd \rightarrow ppp\pi^-$. The solid curve is a fit to the spectrum using Gaussians for the peaks and a fourth order polynomial for the background. The dashed curves show the components. The peak at 30 MeV is events where one proton passed through the body of the target chamber.

yield using an alternative linear fit to the background was 6%. The yield obtained from the fit was corrected for loss of good events due to accidental fast protons firing the associated veto counter. This correction was based on the veto counter rate converted to a probability that it fired for any given event. The maximum correction was 22% with a possible error of 6%.

The validity of the quasifree hypothesis for pion production from deuterium was examined by reconstructing the spectator momentum distribution P_S , which should correspond to that of the deuteron wave function modified by the acceptance of the detectors. Figure 2 shows the experimental P_S distribution which is in good agreement with a Monte Carlo simulation based on the Reid soft core deuteron wave function [10]. An alternate

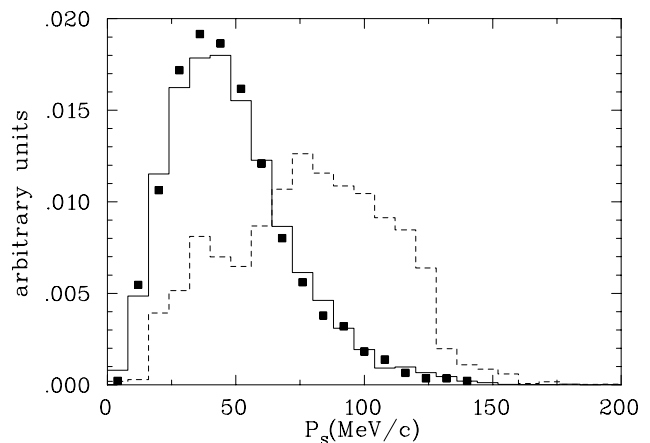


FIG. 2. Comparison of the experimental spectator momentum distribution (points) with Monte Carlo simulations assuming the spectator model (solid line) and a four-body phase space (dashed line).

hypothesis which would yield a momentum distribution for the “spectator” proton governed only by four-body phase space is shown as the dashed curve in Fig. 2. It was found that for all spectrometer field and angle settings, the experimental P_S distribution was incompatible with four-body phase space suggesting that such four-body contributions play a very minor role for our experimental arrangement.

A cut on the relative momentum ΔP of the two protons in the $pp\pi$ c.m. frame, $\Delta P \leq 75$ MeV/c, was implemented to isolate the s -wave diproton final state. The amount of p -wave diproton contamination remaining using this cut was estimated by means of a Monte Carlo simulation based on Handler’s parametrization [11] of s - and p -wave $np \rightarrow pp\pi^-$. The parametrization showed at most a 4% p -wave diproton contamination.

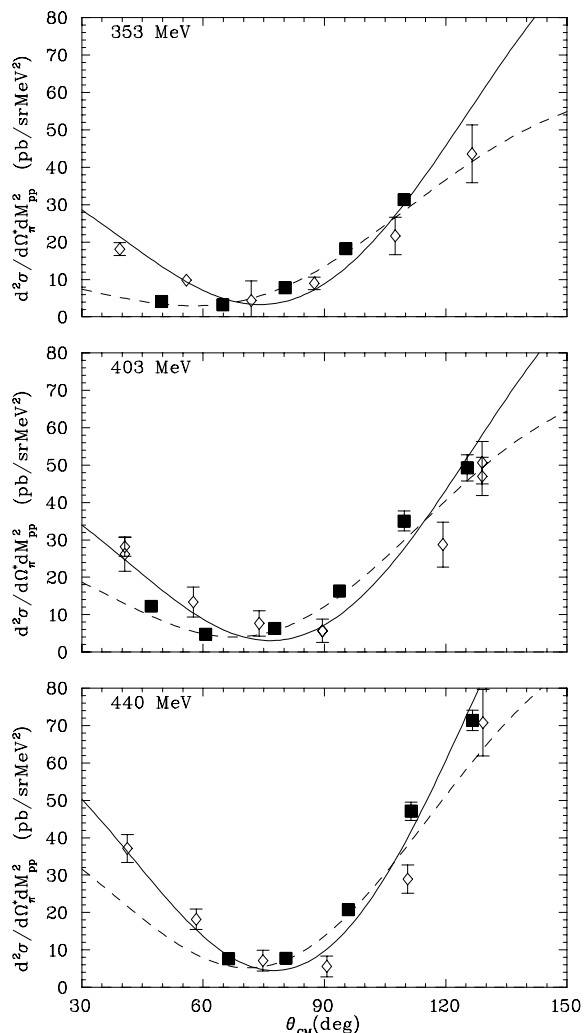


FIG. 3. $d^2\sigma/d\Omega_\pi^*dM_{pp}^2$ for $pn \rightarrow pp(^1S_0)\pi^-$ from this experiment (solid squares). Also shown are the $d\sigma/d\Omega_\pi^*$ results (open diamonds) for ${}^3\text{He}(\pi^-, pn)n$ scaled to compare shapes with the production cross sections. The curves are CCM calculations for production (solid) and absorption (dashed) [13] also scaled to compare shapes with the data.

The free $pn \rightarrow pp\pi^-$ differential cross section was extracted from the $pd \rightarrow ppp\pi^-$ data using the *spectator model* which assumes that (1) the proton in the deuteron is a spectator, influencing the interaction only in terms of the associated Fermi motion of the bound neutron, and (2) that the matrix element for quasifree pion production from a bound neutron is identical to that for free pion production from an unbound neutron at the same two-body energy and momentum transfer. Both the validity of the spectator model and the calibration of the apparatus were checked by reconfiguring the experimental arrangement to extract quasifree $pp \rightarrow d\pi^+$ differential cross sections from $pd \rightarrow d\pi^+n$ data and comparing the results to the well-known free differential cross sections [12]. Such a comparison at several pion angles for $\eta_\pi = 0.66$ yielded an overall normalization error with respect to the Ritchie parametrization [12] of $-3.5 \pm 4.9\%$. Thus, the normalization error is consistent with zero and is within an overall uncertainty of 10% taking a 2σ or 95% confidence level. This level of confidence should apply to the $pd \rightarrow ppp\pi^-$ data if there are no additional systematic uncertainties involved in having an extra particle in the final state.

As the Fermi motion of the target neutron spreads the effective beam energy of the interaction over a range of 40 MeV at the energies investigated here, the $pn \rightarrow pp(^1S_0)\pi^-$ data were binned into 20 MeV wide bins for each beam energy, with only the bin centered at the central energy retained for subsequent analysis. Data corresponding to the wings of the beam energy distribution were discarded. The resulting double differential cross sections as a function of pion c.m. angle, θ_π^* , for the beam energies of this experiment are shown in Fig. 3 and listed in Table I. The error bars shown in the figure and the table are statistical and do not include the 10% normalization uncertainty.

Also shown in Fig. 3 are the ${}^3\text{He}(\pi^-, pn)n$ single differential cross sections for $T_\pi = 37$ [2], 62.5 [3], and 82.8 MeV [3] scaled in order to compare shapes with the pion production data at 353, 403, and 440 MeV, respectively. It is seen that the production data exhibit minima at angles 8° – 13° smaller than those of the absorption data,

TABLE I. $d^2\sigma/d\Omega_\pi^*dM_{pp}^2$ for $pn \rightarrow pp(^1S_0)\pi^-$ in units $\text{pb}(\text{sr})^{-1}(\text{MeV})^{-2}$. The angle θ_π^* is the π^- production angle in the $pp\pi^-$ c.m. frame.

θ_π^* (deg)	$\eta_\pi = 0.66$		$\eta_\pi = 0.92$		$\eta_\pi = 1.06$	
	$d\sigma$	θ_π^* (deg)	$d\sigma$	θ_π^* (deg)	$d\sigma$	θ_π^* (deg)
49.7	4.1(0.2)	47.2	12.3(1.2)	66.3	7.6(0.6)	
64.9	3.3(0.3)	60.6	4.8(0.2)	80.5	7.8(0.5)	
80.3	7.8(0.6)	77.7	6.3(0.3)	95.9	20.8(1.2)	
95.3	18.2(1.2)	93.7	16.3(1.1)	111.4	47.1(2.4)	
109.7	31.3(1.6)	109.7	35.1(2.7)	126.6	71.4(2.7)	
		125.3	49.3(3.5)			

TABLE II. The $\eta_\pi(A1/A2)$ ratio for ${}^3\text{He}(\pi^-, pn)n$ (abs) and $pn \rightarrow pp({}^1S_0)\pi^-$ (prod). $A1$, $A2$, and η_π are explained in the text. The errors specified are statistical and include the correlation errors between the $A1$ and $A2$ fit parameters. The errors do not include any normalization error because such errors cancel out in the ratio.

η_π	$\eta_\pi(A1/A2)$ (abs)	$\eta_\pi(A1/A2)$ (prod)
0.66	-0.59(0.06)	-1.00(0.03)
0.92	-0.48(0.06)	-1.08(0.04)
1.06	-0.53(0.06)	-0.95(0.06)

depending on the energy. In order to properly compare the production and absorption data sets, the data should be compared at the same η_π values. The π absorption data at $T_\pi = 30, 62.5, \text{ and } 82.8$ MeV, have η_π 's of 0.71, 0.95, and 1.11, respectively. These compare quite nicely with the production η_π 's of 0.66, 0.92, and 1.06. Thus, the production and absorption data should be directly comparable as shown. It can be demonstrated from threshold behavior considerations that the ratio $\eta_\pi(A1/A2)$ is constant just above threshold, where $A1$ and $A2$ are the coefficients [2] of the first and second-order Legendre polynomial fits to the cross section data. The ratio can be expected to be more or less constant over the energies of this experiment. The experimental values of $\eta_\pi(A1/A2)$ are shown in Table II. There is a clear distinction between the absorption and the production data. The observed shift has to be entirely attributed to the difference between the absorption and production processes. Furthermore, the position of the cross section minima in the production data is now consistent with the zero crossing angle observed in the analyzing power measurements [7,8].

It can be shown that the displacement of the cross section minima away from 90° is due to an interference between the pion s -wave σ_{11} and the p -wave σ_{01} amplitudes and is a measure of the strength of the isospin one σ_{11} amplitude relative to the dominant isospin zero σ_{01} amplitude. It is obvious from the size of the shift in the minima that the isospin one amplitude is larger in the production data. The reason for this difference between production and absorption is presumably associated with the different nuclear environments for the two processes. A bound $pp({}^1S_0)$ in ${}^3\text{He}$ would be more sensitive to short range correlations, and the ${}^3\text{He}$ nucleus offers the effects of a third nucleon such as a quasifree σ_{10} process, $\pi^- d \rightarrow nn$, followed by charge exchange between one of the neutrons and the spectator proton.

It has been suggested [13] that the relatively large isospin one amplitude seen in the production data could be related to the large pp threshold π^0 production total cross sections. Both involve the same isospin one amplitude. Horowitz *et al.* [14] have used a heavy-meson exchange (HME) mechanism of Lee and Riska [15] to explain the threshold π^0 production behavior. Conversely H ernandez and Oset have used s -wave off-shell rescattering [16] to generate a similar explanation. The HME has been used by Niskanen [13] in a coupled-channels model (CCM) calculation of π^- production, with his recent results shown (scaled) in Fig. 3 to compare with the shapes of the cross sections measured in this work. Interestingly, this calculation is similar in shape with the absorption data, but an earlier calculation (bound diproton) for the absorption data [13] is similar to the production data. Thus, the theoretical situation, at the moment, is not clear.

In summary, the shapes of the differential cross sections of $pn \rightarrow pp({}^1S_0)\pi^-$ (pion production) and $\pi^-(pp) \rightarrow pn$ (pion absorption in ${}^3\text{He}$) are qualitatively different from each other. Theory, both in regard to the isospin one strength and to the absorption/production difference, is not adequate.

The hospitality of E. Vogt and the TRIUMF management is acknowledged by the Tel Aviv University collaborators. We thank W. Kellner and G. Sheffer for technical support. This work was supported in part by the U.S.-Israel Binational Science Foundation, Jerusalem, Israel.

-
- [1] M. Gell-Mann and K.M. Watson, *Annu. Rev. Nucl. Sci.* **4**, 219 (1954).
 - [2] H. Hahn *et al.*, *Phys. Rev. C* **53**, 1074 (1996).
 - [3] K. A. Aniol *et al.*, *Phys. Rev. C* **33**, 1714 (1986).
 - [4] P. Weber *et al.*, *Nucl. Phys.* **A501**, 765 (1989).
 - [5] S. Mukhopadhyay *et al.*, *Phys. Rev. C* **43**, 957 (1991).
 - [6] E. Piasezky *et al.*, *Phys. Rev. Lett.* **57**, 2135 (1986).
 - [7] C. Ponting *et al.*, *Phys. Rev. Lett.* **63**, 1792 (1989).
 - [8] H. Hahn *et al.* (to be published).
 - [9] R. J. Sobie *et al.*, *Nucl. Instrum. Methods Phys. Res., Sect. A* **219**, 501 (1984).
 - [10] R. V. Reid, *Ann. Phys. (N.Y.)* **50**, 411 (1968).
 - [11] R. Handler, *Phys. Rev.* **138**, B1230 (1965).
 - [12] B. G. Ritchie, *Phys. Rev. C* **44**, 533 (1991).
 - [13] J. A. Niskanen, *Phys. Rev. C* **49**, 1285 (1994).
 - [14] C. J. Horowitz *et al.*, *Phys. Rev. C* **49**, 1337 (1994).
 - [15] T. S. H. Lee and D. O. Riska, *Phys. Rev. Lett.* **70**, 2237 (1993).
 - [16] E. H ernandez and E. Oset, *Phys. Lett. B* **350**, 158 (1995).